Analysis of the Electromagnetic Scattering by Perfectly Conducting Convex Polygonal Cylinders

Mario Lucido, *Member, IEEE*, Gaetano Panariello, *Member, IEEE*, and Fulvio Schettino, *Member, IEEE*

***Abstract*—An effective method for the analysis of the scattering by a perfectly conducting convex polygonal cross-section cylinder is presented. The effectiveness stems from the generalization of the Neumann series, factorising the right edge behavior of the electromagnetic field, thus leading to a quickly convergent method. The induced currents, the radar cross section (RCS) and the induced field ratio have been evaluated.**

***Index Terms*—Analytical regularization, cylindrical scatterers, electromagnetic scattering.**

I. Introduction

THE scattering from metallic cylinders has been widely studied in the past years [1]–[11] due to its relevance in electromagnetic theory: radar cross section (RCS) minimization to reduce electromagnetic coupling, aperture blockage effects analysis, scattering of radio beams by local buildings, are just a few examples of applications. Many different approaches, such as finite elements method (FEM) [8], boundary elements method (BEM) [9], the geometrical theory of diffraction (GTD) and the uniform theory of diffraction (UTD) [10], [11], possibly in conjunction with iterative techniques [12] have been applied, depending on the complexity of the structure, and on its electric size. One of the most common approaches, consists in formulating the problem using either the electric or the magnetic field integral equations (EFIE or MFIE), solved by means of the Method of Moments (MoM) [13]. Unfortunately, two problems rise: on one hand, at the frequencies corresponding at the interior resonances of the structure, the matrix obtained by the MoM is singular, in which case the solution is not unique. The problem is even worse, due to the unavoidable truncation of the scattering matrix, leading to an ill-conditioned problem in a wide range about the resonant frequencies. A possible way to overcome this drawback is the use of the combined field integral equation (CFIE), consisting in a linear combination of EFIE and MFIE, or their augmented version [14]. A comparison of the different methods can be found in [15]. On the other hand, when dealing with scatterers with edges, the evaluation of the near-edge currents can be quite difficult because the currents in proximity of the edges can be singular [16], so that the numerical solution of the scattering problem by means of the MoM can become cumbersome. An alternative method, addressing both the aforementioned problems, is the method of analytical regularization (MAR): it consists in either extracting and analytically inverting the singular part of the fullwave operator [17], or using a Galerkin scheme with expansion functions factorizing the right edge behavior of the currents. The Neumann series [17]–[19] is an example of the latter method, applied to equiangular polygonal cross-section cylinders in [20], [21], where the regularization of the problem and the subsequent quick convergence of the method have been pointed out. Moreover, it has been shown that the problem is well-posed even at frequencies arbitrarily close to the theoretical internal resonance frequency of the scatterers [21].

The aim of this paper is the generalization of the Neumann series to analyze convex irregular polygonal cross-section cylinders. The generalization is needed because for irregular polygons the edge behavior is different at the two edges of a side.

Section II deals with the formulation of the problem in the most general case of irregular cross-section cylinders. As usual, for TM incidence the EFIE is used, whilst for TE incidence the MFIE is preferred. Any other incidence can be built by means of TM and TE cases [22]. Section III is devoted to the choice of the expansion functions, generalizing the Neumann series. It is shown that a convenient choice is represented by confluent hypergeometric functions, taking place of Bessel functions in the Neumann series. With such a choice the problem is reduced to the solution of a linear system of algebraic equations. If the cylinder cross section is convex, the elements of the scattering matrix are integrals of a single variable. In Section IV some numerical results are shown, for different cross section shapes. After the convergence of the method has been tested, some comparisons with the literature and with commercial softwares have been performed, with regards to the induced currents, the bistatic RCS and the induced field ratio (IFR) [4]. Finally, some tests about the theoretical internal frequencies of the structure have been performed, to show that the use of the new expansion leads to a well-conditioned problem even at frequencies arbitrarily close to the theoretical internal resonance frequencies of the scatterers. Two Appendixes have been included to remind some relevant properties of confluent hypergeometric functions and to derive their Fourier transform.

II. Formulation of the Problem

Here, the integral equations describing the scattering problem are derived, starting from the vector potential and operating in the spectral domain.

In Fig. 1, the cross section of a perfectly conducting cylinder is plotted: a plane wave impinges onto the cylinder with an angle ϕ with respect to the x axis and orthogonally with respect to the cylinder axis. A local coordinate system (x_i, y_i, z) is also

Manuscript received March 11, 2005; revised November 3, 2005. This work was supported in part by the Italian Ministry of University (MIUR) under a Program for the Development of Research of National Interest (PRIN Grant 2003095273_002).

The authors are with the D.A.E.I.M.I., University of Cassino, Cassino 03043, Italy (e-mail: lucido@unicas.it; panariello@unicas.it; schettino@unicas.it).

Digital Object Identifier 10.1109/TAP.2006.872662

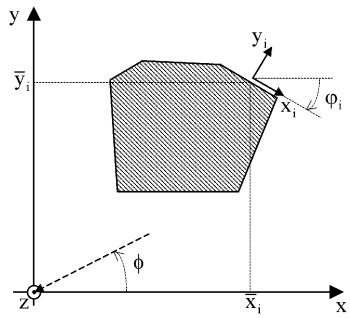

Fig. 1. Geometry of the problem.

sketched in the figure, with the origin at the centre of the ith surface and the y_i axis oriented in the outward direction. If $(\bar{x}_i, \bar{y}_i)$ are the coordinates of the midpoint of the ith surface in the coordinate system (x, y), the relation between the coordinate systems is

$$\begin{cases} x_i(x,y) = (x-\bar{x}_i)\cos\varphi_i + (y-\bar{y}_i)\sin\varphi_i \\ y_i(x,y) = -(x-\bar{x}_i)\sin\varphi_i + (y-\bar{y}_i)\cos\varphi_i. \end{cases} \quad (1)$$

φ_i being the orientation of the ith surface with respect to the x axis.

The surface current distribution can, therefore, be written as

$$\underline{J}(x,y,z) = \underline{J}(x,y) = \sum_{i=1}^{L} \underline{J}_i(x_i(x,y)) \quad (2)$$

where L is the number of faces of the cylinder, $\underline{J}_i(x_i)$ is the surface current on the ith surface and the invariance of the structure with respect to z has been used. The vector potential is then given by

$$\underline{A}(x,y) = \sum_{i=1}^{L} \underline{A}_i(x_i(x,y), y_i(x,y)) \quad (3)$$

where, omitting the dependence from x and y

$$\underline{A}_i(x_i,y_i) = -j\frac{\mu}{4}\int_{-\infty}^{+\infty} \underline{J}_i(x_0) \times H_0^{(2)}\left(k\sqrt{(x_i-x_0)^2+y_i^2}\right) dx_0 \quad (4)$$

μ being the magnetic permeability and k being the wavenumber.

By defining the spatial Fourier transform of $\underline{J}_i(x_i)$ as

$$\tilde{\underline{J}}_i(u) = \frac{1}{2\pi}\int_{-\infty}^{+\infty} \underline{J}_i(x_i) e^{jux_i} dx_i \quad (5)$$

the potential $\underline{A}_i(x_i, y_i)$ can be written as

$$\underline{A}_i(x_i,y_i) = -\frac{j\mu}{4}\int_{-\infty}^{+\infty}\int_{-\infty}^{+\infty} H_0^{(2)}\left(k\sqrt{(x_i-x_0)^2+y_i^2}\right) \times e^{-jux_0} dx_0 \tilde{\underline{J}}_i(u) du \quad (6)$$

which, by using the relevant integral [23]

$$\int_{-\infty}^{+\infty} H_0^{(2)}\left(k\sqrt{(x_i-x_0)^2+y_i^2}\right) e^{-jux_0} dx_0 = 2\frac{e^{-j|y_i|\sqrt{k^2-u^2}}}{\sqrt{k^2-u^2}} e^{-jux_i} \quad (7)$$

leads to

$$\underline{A}(x,y) = -j\frac{\mu}{2}\sum_{i=1}^{L}\int_{-\infty}^{+\infty} \tilde{\underline{J}}_i(u)\frac{e^{-j|y_i|\sqrt{k^2-u^2}}}{\sqrt{k^2-u^2}} e^{-jux_i} du. \quad (8)$$

In (7) the branch has been chosen as follows:

$$\sqrt{k^2-u^2} = \begin{cases} |\sqrt{k^2-u^2}| & \text{if } |u| < k, \\ -j|\sqrt{u^2-k^2}| & \text{if } |u| > k. \end{cases} \quad (9)$$

A. TM Incidence

Let us consider an incident plane wave with TM polarization, namely

$$\underline{E}_{\text{inc}}(x,y) = E_0 e^{-j(k_x x + k_y y)}\hat{z} \quad (10)$$

where $k_x = -k\cos\phi$ and $k_y = -k\sin\phi$. The only non vanishing component of the electric scattered field is, therefore

$$\begin{aligned} E_z(x,y) &= -j\omega A_z(x,y) \\ &= -\frac{\omega\mu}{2}\sum_{i=1}^{L}\int_{-\infty}^{+\infty} \tilde{J}_{\text{iz}}(u) \\ &\quad \times \frac{e^{-j|y_i|\sqrt{k^2-u^2}}}{\sqrt{k^2-u^2}} e^{-jux_i} du \end{aligned} \quad (11)$$

where ω is the angular frequency and the induced current is longitudinal.

By imposing the total electric field to be vanishing on the cylinder surface, a system of L integral equations can be obtained as

$$E_z(x,y)|_{y_j=0} = -\left. E_0 e^{-j(k_x x + k_y y)}\right|_{y_j=0}, \quad |x_j| \le a_j \quad (12)$$

with $j = 1, 2, \ldots L$, $2a_j$ being the width of the jth surface.

B. TE Incidence

In the case of a TE incidence, the magnetic incident field is

$$\underline{H}_{\text{inc}}(x,y) = H_0 e^{-j(k_x x + k_y y)}\hat{z} \quad (13)$$

and the only nonvanishing components of the scattered field are E_x, E_y, and H_z. In such a case, the induced current is transverse, and the scattered magnetic field can be evaluated as

$$\begin{aligned} H_z(x,y) &= \frac{1}{\mu}\nabla\times\underline{A}(x,y)|_z \\ &= -\frac{1}{\mu}\sum_{i=1}^{L}\frac{\partial}{\partial y_i} A_{ix_i}(x_i,y_i) \\ &= \frac{1}{2}\sum_{i=1}^{L}\text{sgn}(y_i)\int_{-\infty}^{+\infty} \tilde{J}_{ix_i}(u) \\ &\quad \times e^{-j|y_i|\sqrt{k^2-u^2}} e^{-jux_i} du \end{aligned} \quad (14)$$

where the signum function

$$\text{sgn}(t) = \begin{cases} -1 & \text{if } t < 0 \\ +1 & \text{if } t > 0 \end{cases} \quad (15)$$

has been introduced.

By imposing the discontinuity of the tangential component of the total magnetic field, namely

$$\hat{n} \times H_z \hat{z}|_S = \underline{J}_S \tag{16}$$

where $\underline{J}_S$ is the surface current distribution on S and $\hat{n}$ is the outward normal, a system of L integral equations can again be obtained

$$H_z(x,y)|_{y_j=0} - J_{x_j}(x_j) = -H_0 e^{-j(k_x x + k_y y)}\Big|_{y_j=0}, |x_j| \le a_j \tag{17}$$

with $j = 1, 2, \ldots L$.

III. Solution of the Problem

In order to reduce the integral equations systems (12) and (17) to algebraic systems of linear equations the Galerkin method can be used. The efficiency of the method is strictly related to the choice of the set of basis and testing functions. In order to analytically regularize the problem in the sense outlined in the Introduction, the selected functions must factorise the right edge behavior prescribed by Meixner conditions [16], improving the convergence of the procedure. For cylinders with a regular polygonal cross section a suitable choice is the Neumann series, namely a series of Bessel functions, adopted in [20] and [21]. In the spatial domain such a series corresponds to a series of Gegenbauer polynomials, multiplied by their weighting function. As a consequence, the expansion functions are orthogonal, and factorise the same (and right) edge behavior on the two edges of a side. On the other hand, when the angles associated to a side are different, namely for irregular cylinders, the edge behavior is different on the two edges. In order to take into account such a behavior it is necessary to select basis functions factorising different behaviors on the two edges. A suitable choice is represented by Jacobi polynomials multiplied by their weighting functions, namely

$$\varphi_n^{(\alpha,\beta)}\left(\frac{x}{c}\right) = \begin{cases} \frac{1}{c}\left(1-\frac{x}{c}\right)^{\alpha}\left(1+\frac{x}{c}\right)^{\beta}\frac{P_n^{(\alpha,\beta)}\left(\frac{x}{c}\right)}{\xi_n^{(\alpha,\beta)}} & \left|\frac{x}{c}\right| \le 1 \\ 0 & \left|\frac{x}{c}\right| > 1 \end{cases} \tag{18}$$

with $n = 0, 1, 2, \ldots$. In (18) $P_n^{(\alpha,\beta)}(\cdot)$ is the Jacobi polynomial of order $n, \alpha, \beta > -1$ are parameters to be chosen so as to factorise the right edge behavior of the unknown function, $2c$ is the width of the generic face and $\xi_n^{(\alpha,\beta)}$ is such that

$$\int_{-c}^{c} (1-x/c)^{\alpha}(1+x/c)^{\beta} \times \left[\frac{P_n^{(\alpha,\beta)}(x/c)}{\xi_n^{(\alpha,\beta)}}\right]^2 \frac{dx}{c} = 1 \quad n = 0, 1, 2, \ldots \tag{19}$$

and is given by

$$\xi_n^{(\alpha,\beta)} = \sqrt{\frac{2^{\alpha+\beta+1}\Gamma(n+\alpha+1)\Gamma(n+\beta+1)}{n!(2n+\alpha+\beta+1)\Gamma(n+\alpha+\beta+1)}}. \tag{20}$$

In order to use the functions defined by (18) in a Galerkin scheme to solve the integral equations derived in the previous section, their Fourier transform is needed. It is possible to show that (see Appendix B)

$$\frac{1}{2\pi c}\int_{-c}^{c} (1-x/c)^{\alpha}(1+x/c)^{\beta}\frac{P_n^{(\alpha,\beta)}(x/c)}{\xi_n^{(\alpha,\beta)}} e^{zx} dx = \bar{\xi}_n^{(\alpha,\beta)}(2cz)^n e^{-cz}\, {}_1F_1(n+\beta+1; 2n+\alpha+\beta+2; 2cz) \tag{21}$$

with $n = 0, 1, 2 \ldots$ and complex values of z, ${}_1F_1(a;b;z)$ being the confluent hypergeometric function of first kind, also known as Kummer function of first kind (see Appendix A) [24]. The coefficients $\bar{\xi}_n^{(\alpha,\beta)}$ are defined in Appendix B.

In particular, when $z = ju$ with $u \in \Re$, relation (21) is the Fourier transform of (18), which will be denoted from now on by

$$\frac{\tilde{\varphi}_n^{(\alpha,\beta)}(cu)}{\bar{\xi}_n^{(\alpha,\beta)}} = (2jcu)^n \times e^{-jcu}\, {}_1F_1(n+\beta+1; 2n+\alpha+\beta+2; 2jcu) \tag{22}$$

with $n = 0, 1, 2, \ldots$

By using the set of functions (18) as testing functions, if the cross section of the cylinder is a convex polygonal the projection is also analytical because it can be reduced to the evaluation of integrals of the kind (21). The system of integral equations in the TM and TE case, reduce, respectively, to

$$\sum_{n=0}^{+\infty}\sum_{i=1}^{L} J_{i_n} \int_{-\infty}^{+\infty} \frac{e^{-jF_{\mathrm{ij}}(u)}}{\sqrt{k^2-u^2}} \tilde{\varphi}_n^{(\alpha_i,\beta_i)}(a_i u) \times \left[\tilde{\varphi}_m^{(\alpha_j,\beta_j)}(a_j G_{\mathrm{ij}}(u))\right]^* du = \frac{2E_0}{\omega\mu} e^{-j(k_x \bar{x}_j + k_y \bar{y}_j)} \left[\tilde{\varphi}_m^{(\alpha_j,\beta_j)}\left(a_j k_{x_j}\right)\right]^* \tag{23}$$

$$\sum_{n=0}^{+\infty}\sum_{i=1}^{L} J_{i_n} \int_{-\infty}^{+\infty} e^{-jF_{\mathrm{ij}}(u)} \tilde{\varphi}_n^{(\alpha_i,\beta_i)}(a_i u) \times \left[\tilde{\varphi}_m^{(\alpha_j,\beta_j)}(a_j G_{\mathrm{ij}}(u))\right]^* du = 2H_0 e^{-j(k_x \bar{x}_j + k_y \bar{y}_j)} \left[\tilde{\varphi}_m^{(\alpha_j,\beta_j)}\left(a_j k_{x_j}\right)\right]^* \tag{24}$$

where $j = 1, 2, \ldots L, m$ is a non negative integer and the star denotes the complex conjugate.

In (23) and (24) J_{i_n} are the expansion coefficients of the current on the ith surface and the following substitutions have been defined

$$F_{\mathrm{ij}}(u) = -\sqrt{k^2-u^2}\, y_i(\bar{x}_j, \bar{y}_j) + u x_i(\bar{x}_j, \bar{y}_j) \tag{25}$$

$$G_{\mathrm{ij}}(u) = \sqrt{k^2-u^2}\sin(\varphi_i - \varphi_j) + u\cos(\varphi_i - \varphi_j) \tag{26}$$

$$k_{x_j} = -k\cos(\phi - \varphi_j). \tag{27}$$

If N functions are used to approximate the current on each side, the scattering matrix associated to (23) and (24) is composed by L^2 square blocks, each with N^2 elements. The block in position (j,i) represents the projection of the scattered field produced by the current distribution on the ith side and evaluated on the jth side.

In order to choose the values of α_i and β_i for $i = 1, 2, \ldots L$ different considerations have to be done for the two incidences.

A. TM Case

In the TM case, due to Meixner conditions, the longitudinal component of the current must exhibit an edge behavior given by

$$J_{iz}(x_i) \underset{x_i \to \pm a_i}{\sim} \left(1 \mp \frac{x_i}{a_i}\right)^{\frac{\psi_i^{\pm} - \pi}{2\pi - \psi_i^{\pm}}} \tag{28}$$

when $\psi_i^{\pm} \leq 3\pi/2$ and $i = 1, 2, \ldots L$, where $\psi_i^{\pm}$ is the angle of the wedge at abscissas $x_i = \pm a_i$. Therefore, in order to factorise the right edge behavior of the currents, the following choices have to be done:

$$\alpha_i = \frac{\psi_i^{+} - \pi}{2\pi - \psi_i^{+}} \text{ and } \beta_i = \frac{\psi_i^{-} - \pi}{2\pi - \psi_i^{-}} \tag{29}$$

with $i = 1, 2, \ldots L$.

B. TE Case

In the TE case, the current on the ith surface has to be finite and nonvanishing. On the other hand, from Maxwell equations one also obtains

$$-\frac{\partial}{\partial x_i} H_z(x, y) = j\omega\varepsilon E_{y_i}(x, y) \text{ with } i = 1, 2, \ldots L \tag{30}$$

which, evaluated on the cylinder surface gives

$$-\frac{\partial}{\partial x_i} J_{ix_i}(x_i) = j\omega\varepsilon E_{y_i}(x, y)|_{y_i = 0} \text{ with } i = 1, 2, \ldots L. \tag{31}$$

As a consequence [16]

$$\frac{\partial}{\partial x_i} J_{ix_i}(x_i) \underset{x_i \to \pm a_i}{\sim} \left(1 \mp \frac{x_i}{a_i}\right)^{\frac{\psi_i^{\pm} - \pi}{2\pi - \psi_i^{\pm}}} \tag{32}$$

when $\psi_i^{\pm} \leq 3\pi/2$ and $i = 1, 2, \ldots L$. Therefore, in order to factorise the right edge behavior of the derivative with respect to x_i of the current density $J_{ix_i}(x_i)$, and, therefore, of the electric field, it has been expanded by using the functions (18) with

$$\alpha_i = \frac{\pi}{2\pi - \psi_i^{+}} \text{ and } \beta_i = \frac{\pi}{2\pi - \psi_i^{-}} \tag{33}$$

with $i = 1, 2, \ldots L$.

C. Numerical Considerations

The factorization of the right edge behavior of the currents, and therefore of the fields, leads to fast converging series, so that only few terms are needed to achieve high accuracy, as it is shown in the following section.

On the other hand, even if small matrices are to be evaluated, the numerical computation of their elements could be cumbersome, so that much attention has to be paid to the evaluation of the integrals. As a matter of fact, it is not difficult to verify that when considering the contributions of two nonadjacent sides, the integrands decay exponentially so that the integrals are quickly converging. In fact, the asymptotic behavior of the integrands $K_{n,m}^{(i,j)}(u)$ of (23) and (24) is

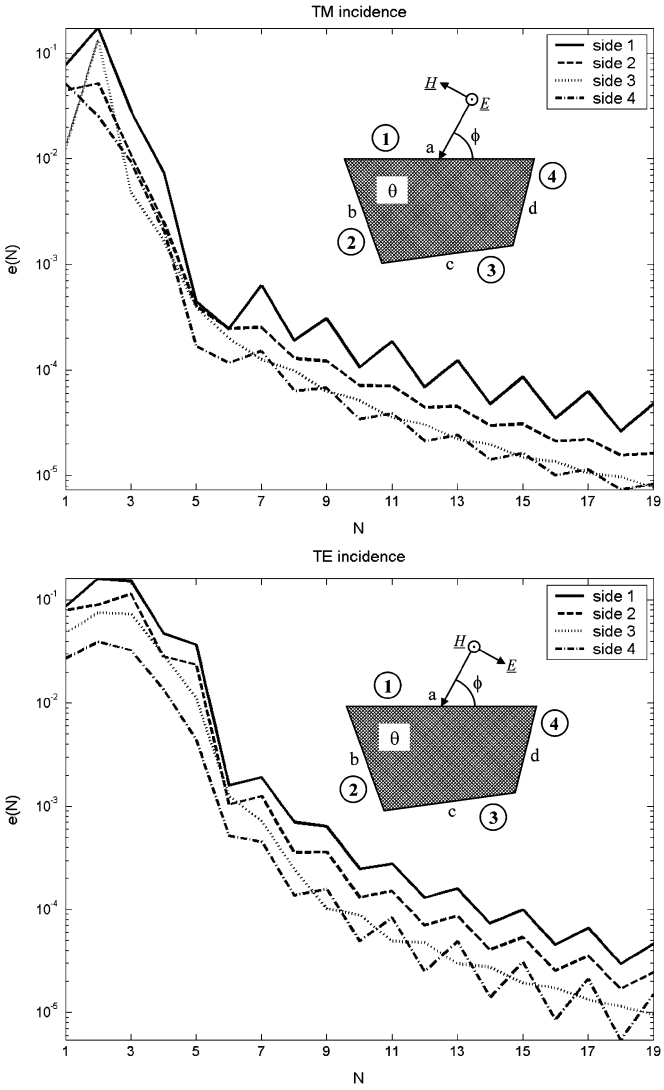

Fig. 2. Normalized truncation error for a quadrangular cross-section cylinder with $a = \lambda, b = 3\lambda/5, c = 3\lambda/4, d = \lambda/2, \vartheta = 70°$ and for $\phi = 60°$. (a) TM incidence. (b) TE incidence.

$$K_{n,m}^{(i,j)}(u) \overset{|u| \to +\infty}{\sim} K_{\infty_{n,m}}^{(i,j)}(u) = \frac{e^{-jux_i(\bar{x}_j, \bar{y}_j)} e^{|u| Y_{ij}}}{(-j|u|)^{\eta}} \tilde{\varphi}_{\infty_n}^{(\alpha_i, \beta_i)}(a_i u) \times \frac{\left[\tilde{\varphi}_{\infty_m}^{(\alpha_j, \beta_j)}\left(a_j u e^{-j\mathrm{sgn}(u)(\varphi_i - \varphi_j)}\right)\right]^*}{e^{a_j |u \sin(\varphi_i - \varphi_j)|}} \tag{34}$$

where η is 0 for TE incidence and 1 for TM incidence, $\tilde{\varphi}_{\infty n}^{(\alpha_i, \beta_i)}(\cdot)$ is the asymptotic behavior of the expansion functions (22), reported in Appendix A, and the function

$$Y_{ij} = y_i(\bar{x}_j, \bar{y}_j) + a_j |\sin(\varphi_i - \varphi_j)| \leq 0 \tag{35}$$

represents the ordinate of the vertex of the jth side closer to the ith side, in the framework of ith side. By simple geometrical considerations it is easy to recognize that the functions defined by (34) are exponentially decaying functions whenever considering nonadjacent sides, in such cases Y_{ij} being less than zero. In the remaining cases it is convenient to extract the asymptotic

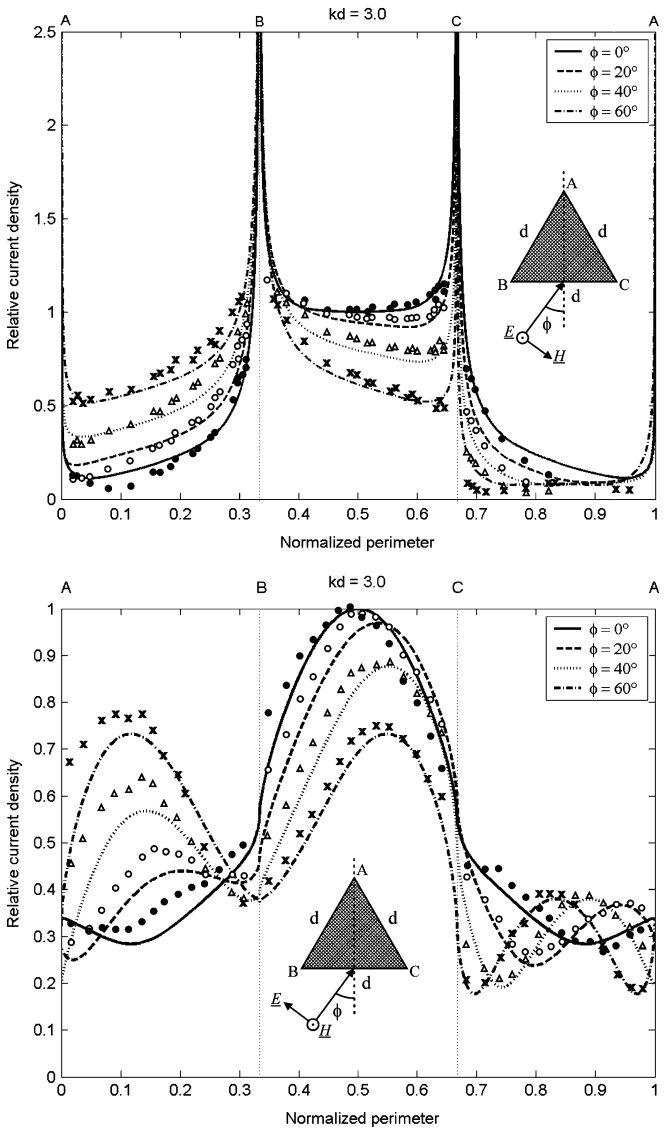

Fig. 3. Surface current density on an equilateral triangular cross-section cylinder in the case $kd = 3.0$ and for different incidence angles. (a) TM incidence $N = 5$. (b) TE incidence $N = 6$. Symbols represent measured data from [3].

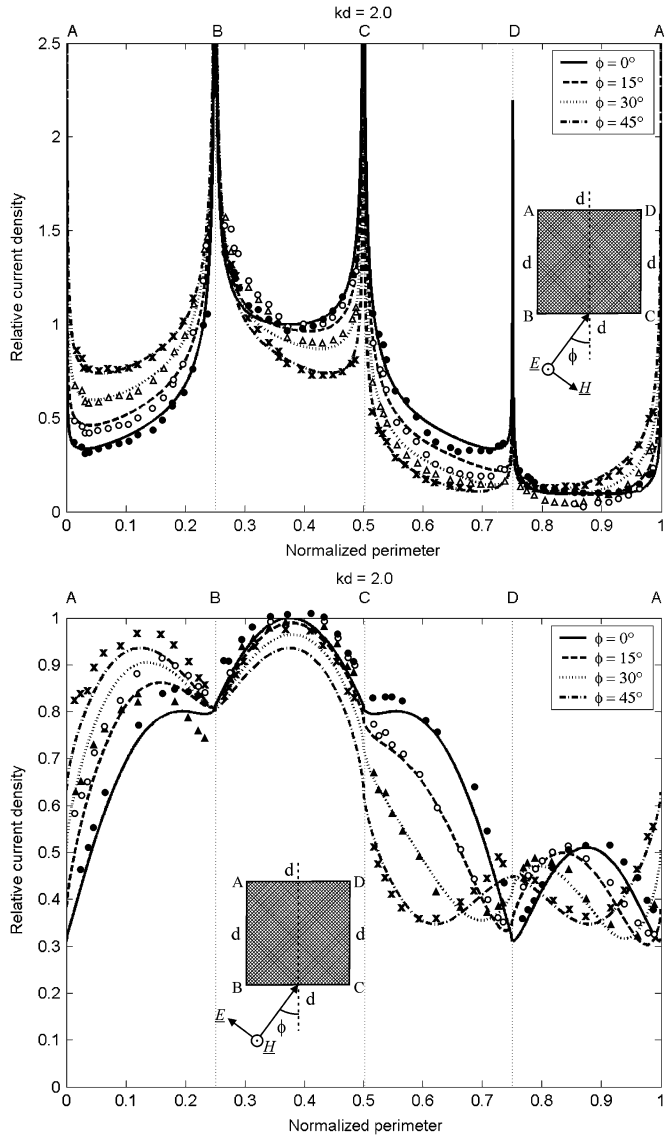

Fig. 4. Surface current density on a square cross-section cylinder in the case $kd = 2$ and for different incidence angles. (a) TM incidence $N = 4$. (b) TE incidence $N = 5$. Symbols represent measured data from [3].

behavior (34) thus obtaining

$$\int_{-\infty}^{+\infty} K_{n,m}^{(i,j)}(u)du = \int_{0}^{M} \Big[K_{n,m}^{(i,j)}(u) + K_{n,m}^{(i,j)}(-u)\Big]\, du + R_{n,m}^{(i,j)}(M) \quad (36)$$

where

$$R_{n,m}^{(i,j)}(M) = \int_{M}^{+\infty} \Big[K_{\infty_{n,m}}^{(i,j)}(u) + K_{\infty_{n,m}}^{(i,j)}(-u)\Big]\, du + O(1/M^3). \quad (37)$$

It is worth noting explicitly that the simple truncation of the integral in (36) would lead to an error of order $O(1/M)$. On the other hand, the integral in (37) can be analytically evaluated as

$$\begin{aligned}\int_{M}^{+\infty} &\Big[K_{\infty_{n,m}}^{(i,j)}(u) + K_{\infty_{n,m}}^{(i,j)}(-u)\Big]\, du \\ &= \frac{j^{\eta} 2^{\alpha_i+\beta_i+\alpha_j+\beta_j+1}}{\pi^2 n!m!\xi_n^{(\alpha_i,\beta_i)}\xi_m^{(\alpha_j,\beta_j)}} \\ &\quad \times \Re\Big\{e^{j\pi[(n+\beta_i+1)\pm(m+\beta_j+1)]} f_{n,m}^{(i,j)}(\beta_i,\beta_j,M) \\ &\quad + f_{n,m}^{(i,j)}(\alpha_i,\alpha_j,M) \\ &\quad + e^{j\pi(n+\beta_i+1)} f_{n,m}^{(i,j)}(\beta_i,\alpha_j,M) \\ &\quad + e^{\pm j\pi(m+\beta_j+1)} f_{n,m}^{(i,j)}(\alpha_i,\beta_j,M)\Big\}. \end{aligned} \quad (38)$$

In (38) $\Re\{\cdot\}$ denotes the real part, and the following substitutions have been done

$$\begin{aligned}&\frac{f_{n,m}^{(i,j)}(\gamma,\delta,M)}{\Gamma(n+\gamma+1)\Gamma(m+\delta+1)} \\ &\quad = \frac{[jZ_{ij}(\gamma,\delta)]^{\gamma+\delta+\eta+1}\Gamma(-\gamma-\delta-\eta-1, jMZ_{ij}(\gamma,\delta))}{(2ja_i)^{\gamma+1}\left[-2ja_je^{-j(\varphi_i-\varphi_j)}\right]^{\delta+1}} \end{aligned} \quad (39)$$

$$\begin{aligned}Z_{ij}(\gamma,\delta) &= x_i(\bar{x}_j,\bar{y}_j) + jy_i(\bar{x}_j,\bar{y}_j) \\ &\quad + r_i(\gamma)a_i - r_j(\delta)a_je^{-j(\varphi_i-\varphi_j)} \end{aligned} \quad (40)$$

$$r_h(\nu) = \begin{cases} -1 & \text{if } \nu = \alpha_h \\ +1 & \text{if } \nu = \beta_h \end{cases} \quad (41)$$

and the upper sign has to be taken if $0 < \varphi_j - \varphi_i < 2\pi$, whilst the lower sign has to be taken if $-\pi < \varphi_j - \varphi_i < \pi$. In (39), $\Gamma(\cdot,\cdot)$ is the incomplete gamma function [24], which can be numerically evaluated very efficiently [25].

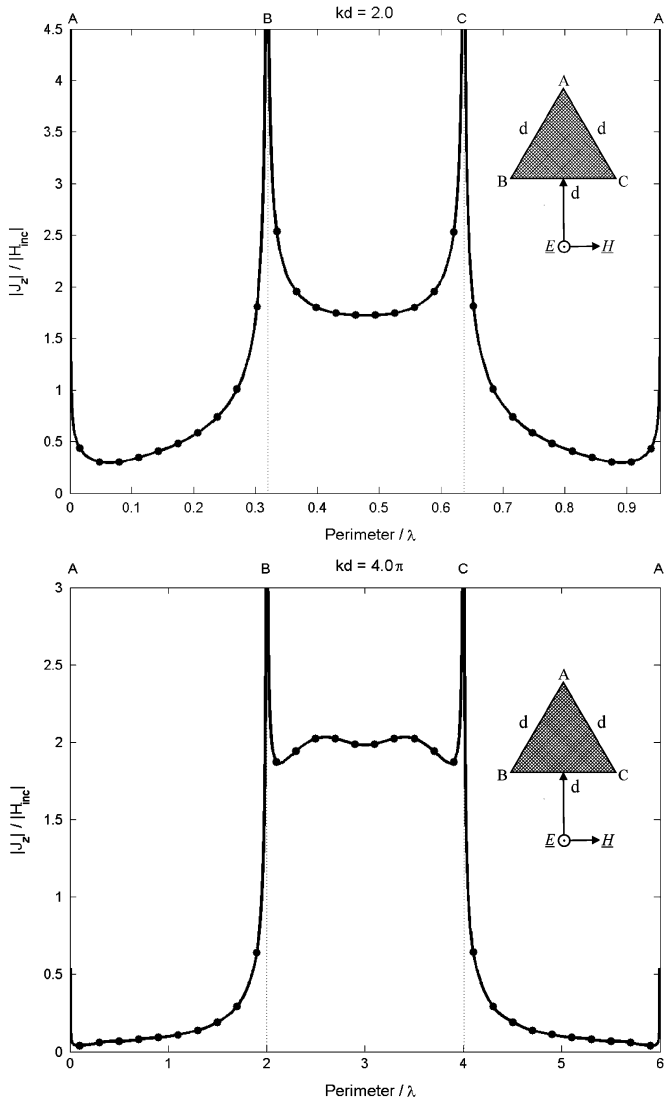

Fig. 5. Surface current density for TM incidence on an equilateral triangular cross-section cylinder for orthogonal incidence. (a) $kd = 2.0, N = 5$. (b) $kd = 4.0\pi, N = 10$. Dots: data from [5].

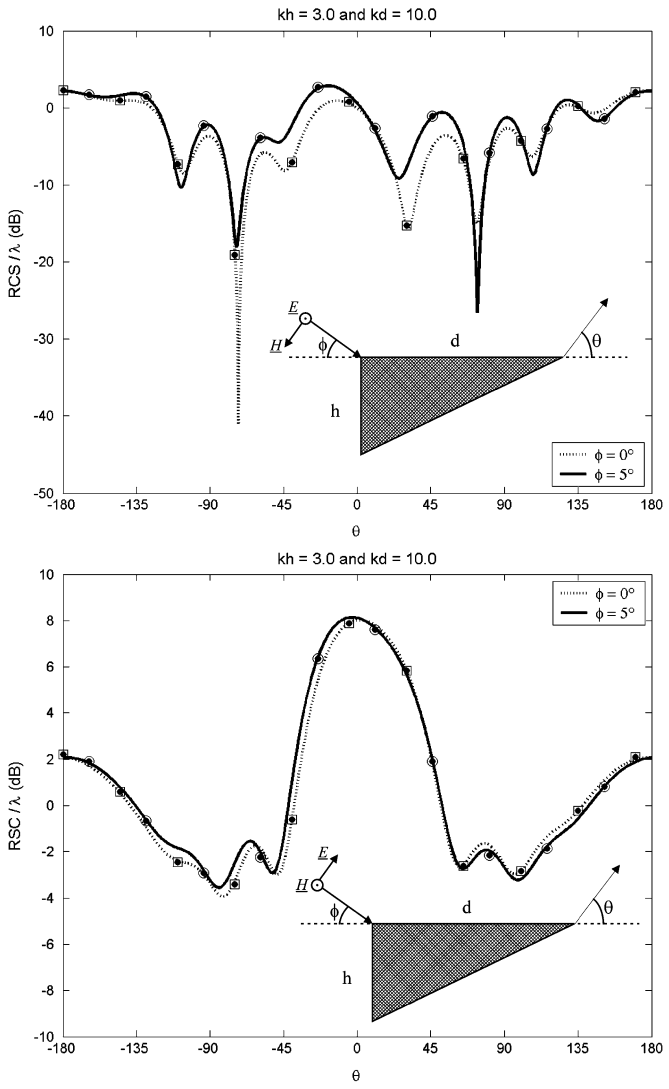

Fig. 6. Normalized RCS of a rectangular triangular cylinder, with angles $\phi = 0°$ and $\phi = 5°$. (a) TM incidence $N = 9$. (b) TE incidence $N = 12$. Other parameters are $kh = 3.0$ and $kd = 10.0$. Dots: CST Microwave Studio simulated data; Squares and Circles: data from [11].

IV. Numerical Results

As a first step the convergence of the method has been tested. In order to evaluate the accuracy improvement when increasing the number of expansion terms, we introduced for each side the following normalized truncation error

$$e(N) = \frac{||J_{N+1} - J_N||}{|H_{\text{inc}}|} \tag{42}$$

where the norm is the usual euclidean norm. In (42), J_N and J_{N+1} are the vectors of the expansion coefficients of the currents evaluated with N and $+1$ terms, respectively. In Fig. 2 the normalized errors are plotted, for a quadrangular cross-section cylinder for both TM and TE incidence. The decaying of the coefficients is very fast, as with $N = 8$ it is possible to reconstruct the unknown current distribution within an accuracy of 10^{-3}. In the following, the same truncation criterion has been adopted and the number of expansion terms used will be reported in the figure caption. Note that the first two coefficients for the TE case are devoted to reconstruct the finite values at edges. It is worth mentioning that the overall method is not very time consuming: in the TM case, which is the most time consuming, 8 expansion terms can be evaluated by means of a C code implementing the numerical procedure outlined in previous Section in 225 s on a Pentium IV 2 GHz, with 512 MB RAM.

The normalized surface current density behaviors in the case of an equilateral triangular cross-section cylinder are plotted in Fig. 3 for different incidence angles, by using only 5 and 6 expansion terms for TM and TE incidence, respectively. In Fig. 4 the surface current density behaviors are plotted in the case of a square cross-section cylinder. In both cases, the agreement with the measurements results reported in [3] by Iizuka and Yen is excellent.

In Fig. 5, the current behavior is plotted in the case of TM incidence when $kd = 2.0$ and $kd = 4.0\pi$ in a scale adequate to compare our results with the ones obtained by Shifman *et al.* [5]. They use an hybrid moment method reconstructing the current by means of multifilament currents in the region far from the edges, and by means of a superposition of the eigensolutions of the infinite-wedge problem near the edges. The number of functions of the two kinds to be used has to be determined empirically: in the cases plotted in Fig. 5 the authors of [5] used 42 and 132 functions, respectively, to obtain accurate results,

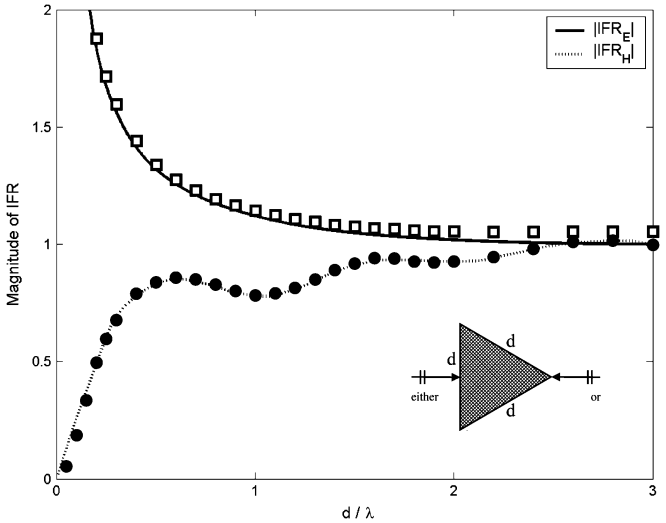

Fig. 7. Induced field ratio of an equilateral triangular cross section as a function of the normalized dimension. Squares and dots represent the data reported in [26]. $N = 14$ and 18 for $\mathrm{IFR_E}$ and $\mathrm{IFR_H}$, respectively.

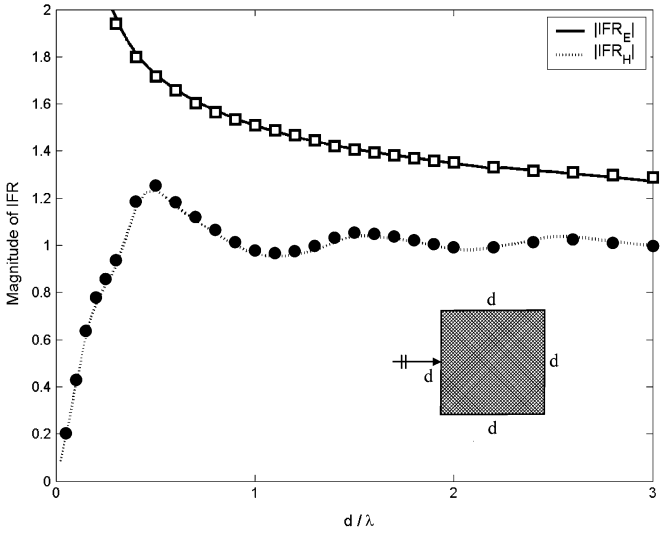

Fig. 8. Induced field ratio of a square cross-section cylinder as a function of the normalized dimension. Squares and dots represent the measured data reported in [4]. $N = 14$ and 18 for $\mathrm{IFR_E}$ and $\mathrm{IFR_H}$, respectively.

while with our method 5 and 10 expansion terms, respectively, are sufficient.

The knowledge of the current distribution allows the evaluation of the scattered far field, and hence of parameters such as the bistatic RCS and the induced field ratio (IFR). In Fig. 6 the RCS of a triangular cross-section cylinder is plotted for both TM and TE incidence, for different incidence angles. Our results are in perfect agreement with those obtained by means of the Uniform geometrical theory of diffraction (UTD) in [11] (squares and circles) and with the simulated data obtained with CST Microwave Studio (dots).

In Figs. 7 and 8 the IFR_E and the IFR_H are plotted for an equilateral triangular cross section and a square cross-section cylinder, with orthogonal incidence as a function of the side length. Our results are comparable with the results showed in [4] and by means of the moment method. It is worth noting that when using the method proposed in [4] and it is necessary to impose the field to be vanishing in interior points in order

TABLE I
EXPANSION TERMS NECESSARY TO OBTAIN THE CORRECT SURFACE CURRENT ON AN EQUILATERAL TRIANGULAR CROSS-SECTION CYLINDER, FOR ORTHOGONAL INCIDENCE. THE THEORETICAL INTERNAL RESONANCE IS AT $d/\lambda = 2/\sqrt{3} = 1.154\,700\,538\,379\,25$ [27]

d/λ	N	
	TM	TE
1.00000	7	8
1.20000	7	9
1.15000	7	9
1.15500	7	9
1.15470	9	11

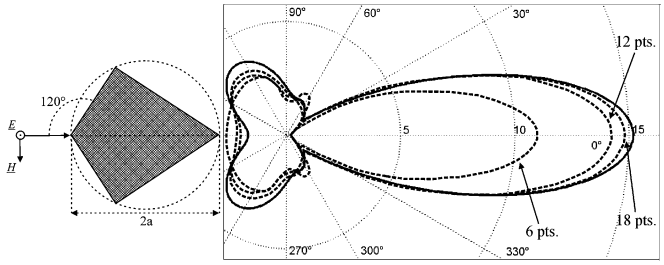

Fig. 9. Normalized bistatic RCS (σ/r) of a quadrilateral cylinder: $ka = 3\sqrt{2}$. Dotted line: results from [28] with 6, 12, and 18 test functions. $N = 5$.

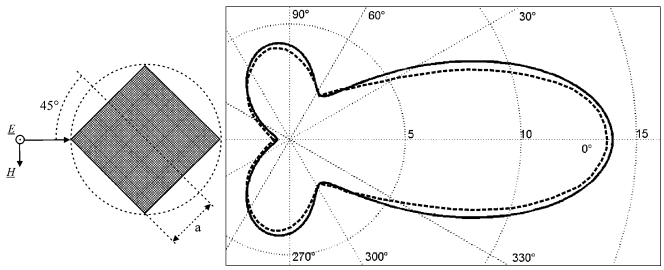

Fig. 10. Normalized bistatic RCS (σ/r) of a square cylinder: $ka = 2$. Dotted line: results from [28]. $N = 5$.

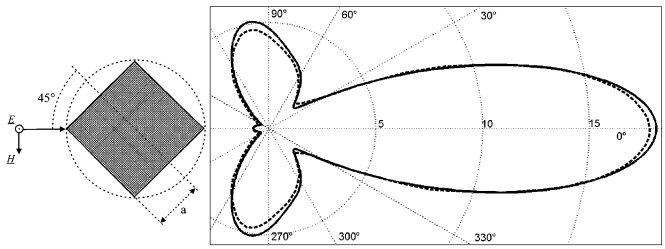

Fig. 11. Normalized bistatic RCS (σ/r) of a sqare cylinder: $ka = 3$. Dotted line: results from [28]. $N = 5$.

to avoid the internal resonances of the cylinder. Our method is immune to this problem when using an adequate number of expansion terms [21]. As an example, in Table I the number of terms necessary to accurately evaluate the induced current are reported for an equilateral triangular cross-section cylinder of side d, when d/λ approaches the first theoretical resonance ($d/\lambda = 2/\sqrt{3}$ [27]).

Finally, in Figs. 9 to 11 the normalized bistatic RCSs of two quadrilateral cylinders have been evaluated and compared with the results obtained in [28] by Bolle and Fye. They subdivide the region exterior to the scatterer into three partially overlapping domains, within each of which complete expansions can be written, and the "point matching" is applied on a surface where all expansions are complete and convergent. Fig. 9 clearly shows that results from [28] tend to our result when increasing

the number of test points. Figs. 10 and 11 also show a good agreement in cases $ka = 2$ and $ka = 3$.

V. Conclusion

In this paper, an effective application of the MoM has been used in the analysis of the scattering by perfectly conducting polygonal cylinders. Simulations have demonstrated that a great reduction of basis functions can be achieved due to the factorization of the right edge behavior of the currents. The method is therefore very appealing for the analysis of conducting structures with edges, and will be extended to concave scatterers in a future work.

Appendix A

The confluent hypergeometric function of first kind, or Kummer function of first kind, with parameters a and b and argument z is defined as [24]

$$ {}_1F_1(a;b;z) = \sum_{n=0}^{+\infty} \frac{\Gamma(n+a)\Gamma(b)Z^n}{\Gamma(a)\Gamma(n+b)z^n n!} \tag{A.1} $$

which is always convergent except when $b = -n, (n \in N)$. In such a case, it has a simple pole at $b = -n$ if $a \neq -m$ or $a = -m$ and $m > n (m \in N)$, and is undefined when $b = -n, a = -m$. It can also be written, when z approaches infinity, as

$$ \begin{aligned} &\frac{{}_1F_1(a;b;z)}{\Gamma(b)} \\ &= \frac{e^{\pm j\pi a} z^{-a}}{\Gamma(b-a)} \left\{ \sum_{n=0}^{R-1} \frac{\Gamma(a+n)\Gamma(1+a-b+n)}{n!\Gamma(a)\Gamma(1+a-b)(-z)^n} + O(|z|^{-R}) \right\} \\ &\quad + \frac{e^z z^{a-b}}{\Gamma(a)} \left\{ \sum_{n=0}^{S-1} \frac{\Gamma(b-a+n)\Gamma(1-a+n)}{n!\Gamma(b-a)\Gamma(1-a)z^n} + O(|z|^{-S}) \right\} \end{aligned} \tag{A.2} $$

where the upper sign has to be chosen when $-\pi/2 < \arg(z) < 3\pi/2$ and the lower sign in the case $-3\pi/2 < \arg(z) < \pi/2$. In (A.2) the remainders are given by

$$ \begin{aligned} O(|z|^{-R}) &= \frac{\Gamma(a+R)\Gamma(1+a-b+R)}{\Gamma(a)\Gamma(1+a-b)\Gamma(R+1)(-z)^R} \\ &\quad \cdot \left[\frac{1}{2} + \frac{1+2b-4a+2z-2R}{8z} + O(|z|^{-2}) \right] \end{aligned} \tag{A.3} $$

and

$$ \begin{aligned} O(|z|^{-S}) &= \frac{\Gamma(b-a+S)\Gamma(1-a+S)}{\Gamma(b-a)\Gamma(1-a)\Gamma(S+1)z^S} \\ &\quad \cdot \left[\frac{2}{3} - b + 2a + z - S + O(|z|^{-1}) \right]. \end{aligned} \tag{A.4} $$

An integral definition of ${}_1F_1(a;b;z)$, in the case $\Re\{b\} > \Re\{a\} > 0$, can also be given

$$ {}_1F_1(a;b;z) = \frac{\Gamma(b)}{\Gamma(b-a)\Gamma(a)} \int_0^1 e^{zt} t^{a-1} (1-t)^{b-a-1} dt. \tag{A.5} $$

Recalling the generic expansion function defined by (22), we are interested into real values of the parameters a and b with $b > a \geq 1/2$. In such a case the expansion obtained combining functions of that kind can be viewed as a generalization of the Neumann series. In fact, recalling the relation between Bessel and Kummer functions [24]

$$ \frac{J_\nu(z)}{z^\nu} = \frac{e^{-jz}}{2^\nu \Gamma(\nu+1)} {}_1F_1\left(\nu + \frac{1}{2}, 2\nu+1, 2jz\right) \tag{A.6} $$

it is not difficult to recognize that the generic term of the Neumann series can be written as

$$ \frac{J_{n+p}(cu)}{(cu)^p} = \frac{j^{-n} \tilde{\varphi}_n^{(p-1/2, p-1/2)}(cu)}{2^{2n+p}\Gamma(n+p+1)\bar{\xi}_n^{(p-1/2,p-1/2)}} \qquad n = 0, 1, 2, \ldots \tag{A.7} $$

Finally, it is worth mentioning the asymptotic behavior of the expansion functions (22) when z approaches 0 or infinity. In the first case, they have a zero of order n, while at infinity their behavior is given by $(n = 0, 1, 2, \ldots)$

$$ \begin{aligned} &\frac{\tilde{\varphi}_n^{(\alpha,\beta)}(cu)}{\bar{\xi}_n^{(\alpha,\beta)}} \underset{\sim}{|u| \to \infty} \frac{\tilde{\varphi}_{\infty n}^{(\alpha,\beta)}(cu)}{\bar{\xi}_n^{(\alpha,\beta)}} \\ &\quad = \frac{e^{\pm j\pi(n+\beta+1)} e^{-jcu}}{\Gamma(n+\alpha+1)(2jcu)^{\beta+1}} + \frac{e^{jcu}}{\Gamma(n+\beta+1)(2jcu)^{\alpha+1}}. \end{aligned} \tag{A.8} $$

Appendix B

The aim of this Appendix is to demonstrate the following relevant result $(n = 0, 1, 2 \ldots)$

$$ \begin{aligned} &\frac{1}{2\pi c} \int_{-c}^{c} (1-x/c)^\alpha (1+x/c)^\beta \frac{P_n^{(\alpha,\beta)}(x/c)}{\xi_n^{(\alpha,\beta)}} e^{zx} dx \\ &\quad = \bar{\xi}_n^{(\alpha,\beta)} (2cz)^n e^{-cz} {}_1F_1(n+\beta+1; 2n+\alpha+\beta+2; 2cz). \end{aligned} \tag{B.1} $$

By using the definition of the Jacobi polynomial [24], the first side of (B.1) can be written as

$$ \begin{aligned} &\frac{1}{2\pi c} \int_{-c}^{c} (1-x/c)^\alpha (1+x/c)^\beta \frac{P_n^{(\alpha,\beta)}(x/c)}{\xi_n^{(\alpha,\beta)}} e^{zx} dx \\ &\quad = \frac{(-1)^n}{2^{n+1}\pi n! \xi_n^{(\alpha,\beta)}} \int_{-1}^{1} \frac{d^n}{dx^n} [(1-x)^{n+\alpha}(1+x)^{n+\beta}] e^{zcx} dx. \end{aligned} \tag{B.2} $$

By iteratively applying the integration by parts, the following formula can be easily obtained

$$ \begin{aligned} &\int_{-1}^{1} \frac{d^n}{dx^n} [(1-x)^{n+\alpha}(1+x)^{n+\beta}] e^{zcx} dx \\ &\quad = \sum_{m=1}^{n} (-zc)^{m-1} \frac{d^{n-m}}{dx^{n-m}} [(1-x)^{n+\alpha}(1+x)^{n+\beta}] e^{zcx} \Big|_{-1}^{1} \\ &\qquad + (-zc)^n \int_{-1}^{1} (1-x)^{n+\alpha}(1+x)^{n+\beta} e^{zcx} dx \end{aligned} \tag{B.3} $$

where, being $\alpha, \beta > -1$, the summation over m vanishes when evaluated at $x = \pm 1$. On the other hand, the integral is proportional to the definition (A.5) of the confluent hypergeometric function, so that (B.1) is readily obtained by setting

$$\bar{\xi}_n^{(\alpha,\beta)} = \frac{2^{\alpha+\beta}\Gamma(n+\alpha+1)\Gamma(n+\beta+1)}{\pi n!\Gamma(2n+\alpha+\beta+2)\xi_n^{(\alpha,\beta)}}. \qquad \text{(B.4)}$$

REFERENCES

[1] K. K. Mei and J. G. Van Bladel, "Scattering by perfectly-conducting rectangular cylinders," *IEEE Trans. Antennas Propag.*, vol. 11, no. 2, pp. 185–192, Mar. 1963.

[2] M. G. Andreasen, "Scattering from parallel metallic cylinders with arbitrary cross sections," *IEEE Trans. Antennas Propag.*, vol. 12, no. 6, pp. 746–754, Nov. 1964.

[3] K. Iizuka and J. L. Yen, "Surface currents on triangular and square metal cylinders," *IEEE Trans. Antennas Propag.*, vol. 15, no. 6, pp. 795–801, Nov. 1967.

[4] W.V.T. Rusch, J. Appel-Hansen, C. A. Klein, and R. Mittra, "Forward scattering from square cylinders in the resonance region with application to aperture blockage," *IEEE Trans. Antennas Propag.*, vol. 24, no. 2, pp. 182–189, Mar. 1976.

[5] Y. Shifman, M. Friedmann, and Y. Leviatan, "Analysis of electromagnetic scattering by cylinders with edges using a hybrid moment method," in *Proc. Inst. Elect. Eng. Microw. Antennas Propag.*, vol. 144, Aug. 1997, pp. 235–240.

[6] H. D. Cheung and E. V. Jull, "Antenna pattern scattering by rectangular cylinders," *IEEE Trans. Antennas Propag.*, vol. 48, no. 10, pp. 1691–1698, Oct. 2000.

[7] V. P. Chumachenko, "Domain-product technique solution for the problem of electromagnetic scattering from multiangular composite cylinders," *IEEE Trans. Antennas Propag.*, vol. 51, no. 10, pp. 2845–2851, Oct. 2003.

[8] T. Roy, T. K. Sarkar, A. R. Djordjevic, and M. Salazar-Palma, "A hybrid method solution of scattering by conducting cylinders (TM Case)," *IEEE Trans. Microw. Theory Tech.*, vol. 44, no. 12, pp. 2145–2151, Dec. 1996.

[9] K. Yashiro and S. Ohkawa, "Boundary element method for electromagnetic scattering from cylinders," *IEEE Trans. Antennas Propag.*, vol. 33, no. 4, pp. 383–389, Apr. 1985.

[10] A. Michaeli, "A uniform GTD solution for the far-field scattering by polygonal cylinders and strips," *IEEE Trans. Antennas Propag.*, vol. 35, no. 8, pp. 983–986, Aug. 1987.

[11] R. Tiberio, G. Manara, G. Pelosi, and R. G. Kouyoumijian, "High-frequency electromagnetic scattering of plane waves from double wedges," *IEEE Trans. Antennas Propag.*, vol. 37, no. 9, pp. 1172–1180, Sep. 1989.

[12] S. Costanzo and G. Di Massa, "Improved spectral iteration technique for the scattering from metallic cylinders," in *Proc. PIERS Progress in Electromagnetics Res. Symp.*, Nantes, France, Jul. 13–17, 1998.

[13] R. F. Harrington, *Field Computation by Moment Methods*. New York: Macmillan, 1968.

[14] A. D. Yaghjian, "Augmented electric- and magnetic-field integral equations," *Radio Sci.*, vol. 16, pp. 987–1001, Nov.–Dec. 1981.

[15] L. M. Correia, "A comparison of integral equations with unique solution in the resonance region for scattering by conducting bodies," *IEEE Trans. Antennas Propag.*, vol. 41, no. 1, pp. 52–58, Jan. 1993.

[16] J. Meixner, "The behavior of electromagnetic fields at edges," *IEEE Trans. Antennas Propag.*, vol. AP-20, pp. 442–446, 1972.

[17] A. I. Nosich, "The method of analytical regularization in wave-scattering and eigenvalue problems: Foundations and review of solutions," *IEEE Antennas Propag. Mag.*, vol. 41, pp. 34–49, 1999.

[18] R. Araneo, S. Celozzi, G. Panariello, F. Schettino, and L. Verolino, "Analysis of microstrip antennas by means of regularization via neumann series," in *Review of Radio Science 1999–2002*, W. R. Stone, Ed. New York: IEEE Press, Wiley Intersci., 2002, pp. 111–124.

[19] K. Eswaran, "On the solutions of a class of dual integral equations occurring in diffraction problems," *Proc. Roy. Soc. London*, ser. A, pp. 399–427, 1990.

[20] E. I. Veliev and V. V. Veremey, "Numerical-analytical approach for the solution to the wave scattering by polygonal cylinders and flat strip structures," in *Analytical and Numerical Methods in Electromagnetic Wave Theory*, M. Hashimoto, M. Idemen, and O. A. Tretyakov, Eds. Tokyo: Science House, 1993.

[21] M. Lucido, G. Panariello, and F. Schettino, "Analytically regularized evaluation of the scattering by perfectly conducting cylinders," *Microw. Opt. Technol. Lett.*, vol. 41, no. 5, pp. 410–414, 2004.

[22] D. S. Jones, *The Theory of Electromagnetism*. New York: Pergamon, 1964.

[23] I. S. Gradshteyn and I. M. Ryzhik, *Table of Integrals, Series, and Products*. London, U.K.: Academic, 1994.

[24] *Handbook of Mathematical Functions, Verlag Harri Deutsch*, 1984. M. Abramowitz, I. A. Stegun.

[25] E. Kostlan and D. Gokhman, "A program for calculating the incomplete Gamma function," in *Internal Rep., Math. Dept.*. Berkeley: Univ. California, Nov. 1987.

[26] W.V.T. Rusch and P. A. Barany, "Forward scattering from cylinders of triangular cross section," *IEEE Trans. Antennas Propag.*, vol. AP-32, p. 1011, 1984. Correction to.

[27] P. L. Overfelt and D. J. White, "TE and TM modes of some triangular cross-section waveguides using superposition of plane waves," *IEEE Trans. Microw. Theory Tech.*, vol. MTT-34, pp. 161–167, 1986.

[28] D. Bolle and D. Fye, "On the application of the 'Point-matching' method to scattering from polygonal cylinders," in *Antennas Propag. Soc. Int. Symp.*, vol. 9, Sep. 1971, pp. 337–340.

Mario Lucido (M'04) was born in Naples, Italy, in 1972. He received the Laurea degree (*summa cum laude*) in electronic engineering in 2000 from the University of Napoli "Federico II," Naples, and the Ph.D. degree in electric and telecommunication engineering in 2004 from the University of Cassino, Cassino, Italy.

Since April 2005, he has been a Researcher with the University of Cassino. His research interests include scattering problems, microwave circuits, and microstrip antennas.

Gaetano Panariello (M'04) was born in Herculaneum, Italy, in 1956. He graduated *summa cum laude* in electronic engineering and received the Ph.D. degree from the University of Napoli "Federico II," Naples, Italy, in 1980 and 1989, respectively.

He was a Staff Engineer with the Antenna Division of the Elettronica SpA until 1984 when he joined the Electromagnetic Research Group of the University "Federico II" of Naples, where from 1990 to 1992, he was a Research Assistant, and from 1992 to 2000, he was an Associate Professor with the Department of Electronic and Telecommunication Engineering, teaching optics, microwave circuit design, and radiowave propagation. In 2000, he joined the Department of Automation, Electromagnetics, Information Engineering and Industrial Mathematics (DAEIMI), University of Cassino, as Full Professor of electromagnetic fields. His research interests include inverse problems, nonlinear electromagnetic, analytical and numerical methods, and microwave circuit design.

Prof. Panariello is a member of the Scientific Committee of the National Inter-University Consortium for Telecommunication (CNIT) and of the Scientific Committee of the Italian Electromagnetic Society (SIEM).

Fulvio Schettino was born in Naples, Italy, in 1971. He received the Laurea degree (*summa cum laude*) in electronic engineering in 1997, and the Ph.D. degree in electronics and computer science in 2001, both from the University of Napoli "Federico II," Naples.

Since June 2001, he has been a Reasearcher with the University of Cassino, Italy. His main research activities concern analytical and numerical techniques for antenna and circuits analysis and adaptive antennas.